THE JOURNAL OF PHYSICAL CHEMISTRY B LETTERS

2009, *113,* 11367–11370
Published on Web 07/29/2009

Tryptophan as a Probe of Photosystem I Electron Transfer Reactions: A UV Resonance Raman Study

Jun Chen, Shana L. Bender,† James M. Keough, and Bridgette A. Barry*

School of Chemistry and Biochemistry and the Petit Institute for Bioengineering and Bioscience, Georgia Institute of Technology, Atlanta, Georgia 30332

Received: July 9, 2009

Photosystem I (PSI) is one of the two membrane-associated reaction centers involved in oxygenic photosynthesis. In photosynthesis, solar energy is converted to chemical energy in the form of a transmembrane charge separation. PSI oxidizes cytochrome c_6 or plastocyanin and reduces ferredoxin. In cyanobacterial PSI, there are 10 tryptophan residues with indole side chains located less than 10 Å from the electron transfer cofactors. In this study, we apply pump−probe difference UV resonance Raman (UVRR) spectroscopy to acquire the spectrum of aromatic amino acids in cyanobacterial PSI. This UVRR technique allows the use of the tryptophan vibrational spectrum as a reporter for structural changes, which are linked to PSI electron transfer reactions. Our results show that photo-oxidation of the chlorophyll *a*/*a*′ heterodimer, P_{700}, causes shifts in the vibrational frequencies of two or more tryptophan residues. Similar perturbations of tryptophan are observed when P_{700} is chemically oxidized. The observed spectral frequencies suggest that the perturbed tryptophan side chains are only weakly or not hydrogen bonded and are located in an environment in which there is steric repulsion. The direction of the spectral shifts is consistent with an oxidation-induced increase in dielectric constant or a change in hydrogen bonding. To explain our results, the perturbation of tryptophan residues must be linked to a PSI conformational change, which is, in turn, driven by P_{700} oxidation.

Long distance electron transfer occurs in many important biological processes, including enzymes involved in mitochondrial electron transfer, photosynthetic energy transduction, and DNA synthesis.[1] In these systems, the protein environment provides a responsive matrix, which controls and regulates the reactions.[2] For example, the phenol and indole side chains of tyrosine[3] and tryptophan,[4] respectively, are redox-active in some enzymes. In addition, the tryptophan side chain can provide an electron tunneling bridge.[4] Previously, changes in the tryptophan ultraviolet (UV) absorption spectrum have been used as a probe of protein dynamics.[5,6] Work on bacteriorhodopsin and the bacterial reaction center suggests that an initial light absorption event can alter protein conformation. Such pretuning of the protein matrix can play an important role in the control of subsequent enzymatic reactions.[5,6]

Photosystem I (PSI) is one of the two membrane-associated reaction centers involved in oxygenic photosynthesis.[7] In photosynthesis, solar energy is converted to chemical energy in the form of a transmembrane charge separation. PSI catalyzes the transfer of an electron from plastocyanin or a cytochrome c_6 to ferredoxin.[8] Electron transfer is initiated by photoexcitation of the primary electron donor, which is most likely a monomeric accessory chlorophyll (chl).[9] As shown in Figure 1, the electron is then transferred through a series of acceptor molecules, which are named A_0 (chlorophyll *a*), A_1 (phylloquinone), F_x (iron sulfur cluster), F_A (iron sulfur cluster), and F_B (iron sulfur cluster).

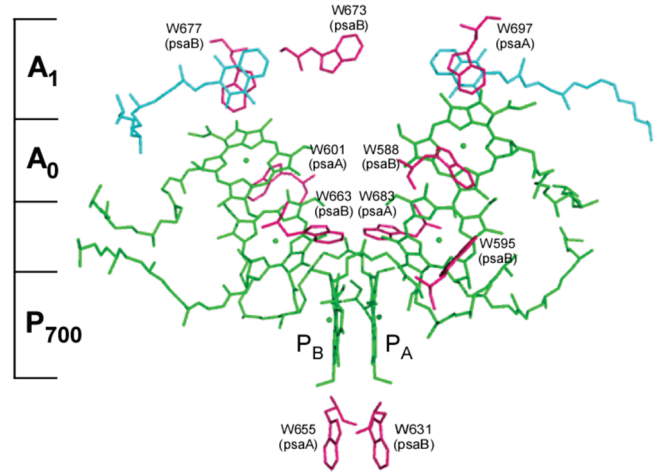

Figure 1. P_{700}, A_0, and A_1 electron transfer cofactors and their neighboring (<10 Å) tryptophan residues in cyanobacterial PSI (PDB access code: 1JB0).[13] The F_X, F_A, and F_B electron acceptors are not shown. Residue numbers are based on the *Synechococcus elongatus* sequence.

There are two A_0 and A_1 acceptor molecules, arranged with approximate C_2 symmetry. It has been proposed that both sets of electron acceptors, called the A and B branches, are active in PSI electron transfer.[10] The primary chlorophyll donor oxidizes P_{700}, a chlorophyll *a*/*a*′ heterodimer, which serves as the terminal electron donor in the PSI reaction center.[11,12] In the cyanobacterial PSI monomer, there are 10 tryptophan residues (Figure 1) with indole side chains less than 10 Å from the redox-active cofactors.[13]

* To whom correspondence should be addressed. E-mail: bridgette.barry@chemistry.gatech.edu.
† Current address: Chemistry Division, Argonne National Laboratory, 9700 S. Cass Ave., Argonne, Illinois 60439.

10.1021/jp906491r CCC: $40.75

To obtain more information concerning redox-linked structural changes in cyanobacterial PSI,[14−18] we employ here a novel UV resonance Raman (UVRR) microprobe technique.[19] UVRR spectroscopy provides an incisive method with which to monitor environmental and structural changes in tryptophan.[20−22] Excitation in the UV enhances Raman scattering from aromatic amino acid residues, and the Raman experiment provides a high resolution spectrum, which is sensitive to protein structural perturbations.[23−28] With this approach, changes in hydrogen bonding, protonation state, and dielectric constant can be detected. In this paper, we show that electron transfer reactions in PSI perturb tryptophan residues, which act as sensors of protein conformational changes.

Materials and Methods

PSI trimers from *Synechocystis* sp. PCC 6803 cultures were purified as previously described.[14−18,29] *Synechocystis* PCC 6803 cultures were grown on solid media containing BG-11,[30,31] 5 mM glucose, 6 mM $Na_2S_2O_3$, and 5 mM TES-NaOH, pH 8.0. Liquid cultures were grown in BG-11, 5 mM glucose, 5 mM TES-NaOH, pH 8.0, and were bubbled with sterile air. Trimeric PSI was purified by ion exchange chromatography. After purification, samples were dialyzed against 5 mM HEPES-NaOH and 0.04% *n*-dodecyl-*β*-*d*-maltopyranoside, pH 7.5, and concentrated to 1.3 mg of chlorophyll/mL using an Amicon (Bedford, MA) Ultra 100K MWCO centrifugal filter device. Chlorophyll quantitation was conducted in 100% methanol.[31,32]

To assess enzyme activity, the steady-state oxygen consumption rate was monitored at 25 °C through the use of a Clark-type oxygen electrode (YSI Inc., Yellow Springs, OH).[16,29] Air-saturated water was used as an oxygen standard. The PSI sample, corresponding to 20 μg of chlorophyll, was diluted into a buffer containing 50 mM MES-NaOH (pH 6.5), 10 mM NaC1, 25 mM $CaC1_2$, 1.0 M sucrose, 0.1 mM sodium 2,6-dichloroindophenolate hydrate (DCPIP), 5 mM sodium L-ascorbate, and 0.1 mM methyl viologen dichloride. The total assay volume was 1.5 mL. Continuous red light illumination was provided with an optical fiber and a red-filtered light source (Dolan-Jenner, model 180, Boxborough, MA). The steady-state oxygen consumption rates of the PSI samples were ∼200 μmol of O_2 (mg of chlorophyll)$^{-1}$ h^{-1} before and after the UVRR measurements.

UVRR measurements were conducted at room temperature using 229 nm as the Raman probe wavelength.[19] This UV probe wavelength is expected to resonantly enhance the vibrational signal of tryptophan and tyrosine. The spectral resolution was 8 cm^{-1}. The precision, which reflects the repeatability of successive frequency measurements at an identical grating position, was less than 1.0 cm^{-1}. To prevent sample damage from the UV irradiation, the PSI samples were recirculated through a nozzle (∼120 μm inner diameter) to form a jet stream, which passed through the UV laser spot at a high flow rate (∼4.5 m/s).[19] For the pump−probe difference measurements, a 10 mW, 633 nm pump beam with 1.0 mm diameter was used to induce light-induced charge separation prior to UV excitation. The red laser spot was displaced from the UV Raman probe and was used to illuminate the sample just before the Raman excitation. The transit time through the red pump beam was estimated as 200−250 μs.

Electron paramagnetic resonance (EPR) analysis was conducted at room temperature with a Bruker EMX spectrometer and a Bruker ER4102ST cavity (TE_{102}).[29,33] The sample was placed in a quartz EPR flat cell. Continuous red light illumination was provided with an optical fiber and a red-filtered and heat-filtered light source. The spectral conditions for field-swept EPR spectra were the following: microwave frequency, 9.819 GHz; microwave power, 20.2 mW; modulation amplitude, 5.0 G; sweep time, 167.77 s; receiver gain, 1.12×10^5; and time constant, 1310.72 ms. Two sets of data were collected and averaged.

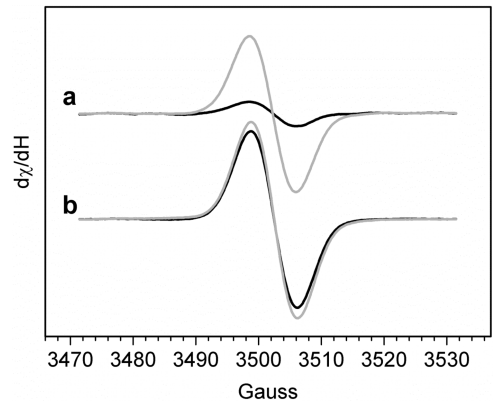

Figure 2. Room temperature P_{700}^+ EPR spectrum in PSI, containing no exogenous electron acceptors (a) and in PSI, containing 0.75 mM potassium ferricyanide (b). In each panel, the black spectrum was recorded in the dark; the gray spectrum was recorded under red light illumination, which was provided with a fiber-optic and a red-filtered tungsten light source (Dolan-Jenner, model 180). The spectra are the average of two data sets. The chlorophyll concentration was 0.5 mg/mL.

Results and Discussion

In these PSI samples, visible illumination results in the generation of the charge separated state, $P_{700}^+F_A/F_B^-$. The formation of $P_{700}^+F_A/F_B^-$ is on a submicrosecond time scale,[34,35] and the $P_{700}^+F_A/F_B^-$ charge recombination time is on the order of milliseconds.[35−37] Therefore, the stable generation of P_{700}^+ under visible illumination is expected and can be monitored by room temperature EPR spectroscopy.[29] Under these conditions, the EPR signal from the reduced iron sulfur cluster is not detectable.[38] Figure 2a shows the P_{700}^+ EPR spectrum in the dark (black line) or under red light illumination (gray line). As expected,[29] the EPR signal of P_{700}^+ has a *g* value of 2.003 and a hyperfine splitting of 7 G. The P_{700}^+ signal increases in amplitude under illumination, as expected if the charge separated state, $P_{700}^+F_A/F_B^-$, is generated.

To acquire the UVRR spectrum of PSI, a 229 nm UV laser line was used as the Raman excitation source. A jet flow sample cell and a red (633 nm) pump−UV (229 nm) probe difference method were used to monitor perturbations to tryptophan vibrational bands, caused by PSI electron transfer reactions. Because tryptophan exhibits a strong 218 nm B_b electronic transition,[39] tryptophan vibrational signals are resonantly enhanced with 229 nm excitation.[39,40]

Figure 3a presents the 229 nm UVRR spectrum of PSI. Prominent bands at 759, 875, 1011, 1175, 1360, 1552, and 1615 cm^{-1} are observed. Comparison with the 229 nm UVRR spectra of tryptophan and tyrosine solutions (Figures S1 and S2 in the Supporting Information) shows that the PSI UVRR spectrum is dominated by tryptophan and tyrosine vibrational bands. Table S1 in the Supporting Information and Figure 3a list the assignments of the tyrosine and tryptophan vibrational bands, which are observed in PSI.[39,41] Note that the observed PSI bands do not arise from chlorophyll. At 229 nm, the chlorophyll Raman spectrum is not expected to be resonantly enhanced, and

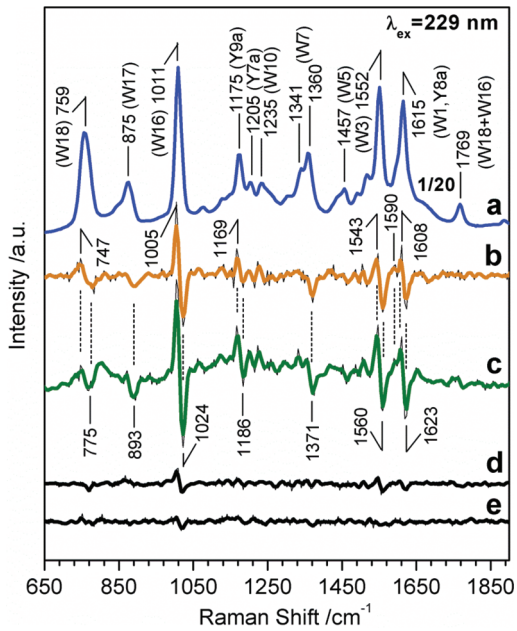

Figure 3. UVRR spectra of PSI acquired with a 450 μW, 229 nm probe beam and an exposure time of 21 min. When employed, the power of a 633 nm pump beam was 10 mW. The data in part a are a 229 nm probe-only PSI spectrum. The data in part b are a (633 nm) pump-minus-(229 nm) probe PSI difference spectrum, corresponding to generation of the light-induced $P_{700}^{+}F_A/F_B^{-}$-minus-$P_{700}F_A/F_B$ state. The data in part c are a 229 nm probe-only P_{700}^{+}-minus-P_{700} spectrum, resulting from subtraction of data recorded in the presence and absence of 3 mM potassium ferricyanide. The controls in parts d and e, in which no vibrational bands are expected, were recorded with the 229 nm probe alone and were generated by subtraction of the last 9 min from the first 9 min of data collection on the same sample. The control samples contained PSI (d) or PSI with 3.0 mM potassium ferricyanide (e). For presentation purposes, the intensity of part a was divided by 20. All of the spectra are the average of three data sets. The orange, green, and black lines represent a three-point smoothed fit to the Raman data. The chlorophyll concentration was 1.3 mg/mL.

frequencies and amplitudes in the chlorophyll Raman spectrum are distinct from the spectra of tyrosine and tryptophan.[19]

To establish a charge separation in the PSI samples, a 633 nm laser beam was employed. The red laser spot was displaced from the UV Raman probe and was used to illuminate the sample just before Raman excitation. Subtraction of probe-only data from the pump-plus-probe data reveals the alterations in the Raman spectrum caused by the charge separation, $P_{700}^{+}F_A/F_B^{-}$-minus-$P_{700}F_A/F_B$. Figure 3b shows such a light-induced difference spectrum of PSI. Comparison with Figure 3a demonstrates that frequency shifts of tryptophan vibrational bands are observed.

The spectral changes observed in Figure 3b are specific for red illumination because these band shifts are not significant when the red pump beam is not employed (Figure 3d). The negative control in Figure 3d also shows that any 229 nm actinic effect is negligible. In addition, comparison of Figure 3b to the negative control (Figure 3d) shows that the observed spectral changes are not caused by UV-induced sample damage.

The spectral perturbations observed in Figure 3b may be caused by oxidation of P_{700} or by reduction of the F_A/F_B iron sulfur cluster. To distinguish between these two possibilities, PSI was treated with potassium ferricyanide. As shown in Figure 2b, the amplitude of the P_{700}^{+} EPR signal is similar in the dark (black line) and under red light illumination (gray line), indicating that potassium ferricyanide oxidizes P_{700} in the dark. Under these conditions, F_A/F_B remains in the oxidized form. As indicated by comparison of Figure 3b and c, chemical oxidation in the dark (Figure 3c) or photo-oxidation (Figure 3b) gives a similar difference UVRR spectrum. The spectral perturbations observed in Figure 3c are significant when compared to a negative subtraction control (Figure 3e), in which one-half of a data set was subtracted from the other half of that same set. These results demonstrate that chemical or photoinduced oxidation of P_{700} perturbs the environment of PSI tryptophan residues. The intensity of the difference signal in Figure 3c is ~3% of the total Raman intensity (Figure 3a). There are 75 tryptophan residues in a PSI monomer.[13] Thus, our data predict that two or more tryptophan residues contribute to the difference spectrum.

Chemical or photo-oxidation causes intensity changes and frequency shifts in tryptophan vibrational modes (Figure 3b and c). In these difference spectra, a negative band is observed at 893 cm^{-1}, 18 cm^{-1} upshifted from the average frequency of 875 cm^{-1} (W17) for PSI tryptophans (Figure 3a). The corresponding positive component for this W17 band must have lower intensity and is not observed. It is known that the frequency of the W17 band reflects H-bonding strength at the indole nitrogen. For this band, lower frequencies correspond to stronger hydrogen bonding, and a W17 frequency has been reported at ~883 cm^{-1} with no hydrogen bonding.[42] The observation that P_{700} oxidation perturbs a tryptophan band at 893 cm^{-1} indicates that, in the dark, the perturbed PSI tryptophan is only weakly or not hydrogen bonded.

The difference spectra (Figure 3b and c) also exhibit a negative W7 band at 1371 cm^{-1}, which has an unusual blue shift of 11 cm^{-1}, compared to the average PSI frequency (Figure 3a). For this normal mode, such a frequency perturbation is likely to arise from a steric repulsion between the indole ring and its environment. A similar frequency was observed for a tryptophan W7 band in bacteriorhodopsin. In that case, the frequency shift was attributed to repulsion between the indole ring and the methyl groups of the retinal chromophore.[43,44] Again, the expected positive band is not observed with significant intensity.

In Figure 3b and c, derivative-shaped spectral features are observed at 747 (+)/775 (−) cm^{-1} (W18), 1005 (+)/1024 (−) cm^{-1} (W16), 1543 (+)/1560 (−) cm^{-1} (W3), and 1608 (+)/1623 (−) cm^{-1} (W1) modes. These bands exhibit downshifts in frequency when P_{700} is oxidized, suggesting a change in the tryptophan environment. Furthermore, in the dark, the observed frequencies of most of these bands are upshifted relative to the average frequency of PSI tryptophans, again suggesting a unique protein environment for the perturbed tryptophans (Figure 3a).

In summary, the UVRR experiment reveals that two or more tryptophan side chains are perturbed by P_{700} oxidation. The perturbed tryptophan side chains are only weakly or not hydrogen bonded and are located in an environment in which there is steric repulsion. As shown in Figure 1, Trp 663 (psaB) and Trp 683 (psaA) are possible candidates for the perturbed tryptophans. These two tryptophans are in a hydrophobic environment and are not extensively hydrogen bonded. The indole rings are ~7 Å from the P_{700} Mg atoms, and the residues are ~3 Å from one of the P_{700} methyl groups.[13] However, other possible assignments cannot be excluded at this time.

When P_{700} is oxidized, an average 20 cm^{-1} frequency downshift of the W18, W16, W3, and W1 modes, originating from the perturbed tryptophans, is observed. These normal modes involve benzene/pyrrole breathing (W18 and W16), pyrrole ring stretching (W3), and benzene ring stretching (W1). We consider a vibrational Stark shift, due to the generation of

a positive charge on P_{700}, as an unlikely explanation for this spectral perturbation. The magnitude of a vibrational Stark effect depends on the relative orientations of the electric field and the transition dipole.[45,46] Therefore, a vibrational Stark effect is unlikely to have such a uniform effect on four normal modes, which involve such different nuclear displacements. However, model studies have shown that increases in solvent dielectric constant and hydrogen bonding strength lower the frequencies of these bands.[47−49] We conclude that a change in internal dielectric constant or hydrogen bonding is linked to a protein conformational change. To explain our results, this protein structural change must be driven by P_{700} oxidation. Previous FT-IR studies have detected a light-induced distribution in hydrogen bonding to P_{700},[15,18] which is also consistent with an oxidation-induced protein structural change.

In conclusion, pump−probe difference UVRR investigations reveal that oxidation of P_{700} is coupled with a dielectric or hydrogen bonding change, which alters the environment of PSI tryptophan residues. Such redox-linked changes may play an important role in control of PSI electron transfer reactions.

Acknowledgment. This project was supported by NSF MCB 08-42246 and Award Number R01GM043273 from the National Institute of General Medical Sciences and the National Eye Institute. The content is solely the responsibility of the authors.

Supporting Information Available: 229 nm probe UVRR spectra of tryptophan and tyrosine solutions and table of vibrational assignments for PSI. This material is available free of charge via the Internet at http://pubs.acs.org.

References and Notes

(1) Stubbe, J.; Nocera, D. G.; Yee, C. S.; Chang, M. C. Y. *Chem. Rev.* **2003**, *103*, 2167.
(2) Gray, H. B.; Winkler, J. R. *Q. Rev. Biophys.* **2003**, *36*, 341.
(3) Barry, B. A.; Babcock, G. T. *Proc. Natl. Acad. Sci. U.S.A.* **1987**, *84*, 7099.
(4) Shih, C.; Museth, A. K.; Abrahamsson, M.; Blanco-Rodriguez, A. M.; Di Bilio, A. J.; Sudhamsu, J.; Crane, B. R.; Ronayne, K. L.; Towrie, M.; Vlcek, A.; Richards, J. H.; Winkler, J. R.; Gray, H. B. *Science* **2008**, *320*, 1760.
(5) Schenkl, S.; van Mourik, F.; van der Zwan, G.; Haacke, S.; Chergui, M. *Science* **2005**, *309*, 917.
(6) Wang, H.; Lin, S.; Allen, J. P.; Williams, J. C.; Blankert, S.; Laser, C.; Woodbury, N. W. *Science* **2007**, *316*, 747.
(7) Nelson, N.; Yocum, C. F. *Annu. Rev. Plant Biol.* **2006**, *57*, 521.
(8) Golbeck, J. H. *Photosynth. Res.* **1999**, *61*, 107.
(9) Holzwarth, A. R.; Muller, M. G.; Niklas, J.; Lubitz, W. *Biophys. J.* **2006**, *90*, 552.
(10) Guergova-Kuras, M.; Boudreaux, B.; Joliot, A.; Joliot, P.; Redding, K. *Proc. Natl. Acad. Sci. U.S.A.* **2001**, *98*, 4437.
(11) Fromme, P.; Jordan, P.; Krauβ, N. *Biochim. Biophys. Acta* **2001**, *1507*, 5.
(12) Grotjohann, I.; Fromme, P. *Photosynth. Res.* **2005**, *85*, 51.
(13) Jordan, P.; Fromme, P.; Witt, H. T.; Klukas, O.; Saenger, W.; Krauβ, N. *Nature* **2001**, *411*, 909.
(14) Noren, G. H.; Boerner, R. J.; Barry, B. A. *Biochemistry* **1991**, *30*, 3943.
(15) Kim, S.; Barry, B. A. *J. Am. Chem. Soc.* **2000**, *122*, 4980.
(16) Kim, S.; Sacksteder, C.; Barry, B. A. *Biochemistry* **2001**, *40*, 15384.
(17) Bender, S. L.; Keough, J. M.; Boesch, S. E.; Wheeler, R. A.; Barry, B. A. *J. Phys. Chem. B* **2008**, *112*, 3844.
(18) Bender, S. L.; Barry, B. A. *Biophys. J.* **2008**, *95*, 3927.
(19) Chen, J.; Barry, B. *Photochem. Photobiol.* **2008**, *84*, 815.
(20) Kim, J. E.; Pan, D. H.; Mathies, R. A. *Biochemistry* **2003**, *42*, 5169.
(21) El-Mashtoly, S. F.; Yamauchi, S.; Kumauchi, M.; Hamada, N.; Tokunaga, F.; Unno, M. *J. Phys. Chem. B* **2005**, *109*, 23666.
(22) Shafaat, H. S.; Leigh, B. S.; Tauber, M. J.; Kim, J. E. *J. Phys. Chem. B* **2009**, *113*, 382.
(23) Ames, J. B.; Ros, M.; Raap, J.; Lugtenburg, J.; Mathies, R. A. *Biochemistry* **1992**, *31*, 5328.
(24) Rodgers, K. R.; Su, C.; Subramaniam, S.; Spiro, T. G. *J. Am. Chem. Soc.* **1992**, *114*, 3697.
(25) Asher, S. A. *Anal. Chem.* **1993**, *65*, A201.
(26) Nagai, M.; Wajcman, H.; Lahary, A.; Nakatsukasa, T.; Nagatomo, S.; Kitagawa, T. *Biochemistry* **1999**, *38*, 1243.
(27) Okada, A.; Miura, T.; Takeuchi, H. *Biochemistry* **2001**, *40*, 6053.
(28) Sanchez, K. M.; Neary, T. J.; Kim, J. E. *J. Phys. Chem. B* **2008**, *112*, 9507.
(29) Sacksteder, C. A.; Bender, S. L.; Barry, B. A. *J. Am. Chem. Soc.* **2005**, *127*, 7879.
(30) Rippka, R.; Derulles, J.; Waterbury, J. B.; Herdman, M.; Stanier, R. *J. Gen. Microbiol.* **1979**, *111*, 1.
(31) Barry, B. A. *Methods Enzymol.* **1995**, *258*, 303.
(32) Lichtenthaler, H. K. *Methods Enzymol.* **1987**, *148*, 350.
(33) Kim, S.; Ayala, I.; Steenhuis, J. J.; Gonzalez, E. T.; Razeghifard, M. R.; Barry, B. A. *Biochim. Biophys. Acta* **1998**, *1366*, 330.
(34) Setif, P. Q. Y.; Bottin, H. *Biochemistry* **1994**, *33*, 8495.
(35) Brettel, K. *Biochim. Biophys. Acta* **1997**, *1318*, 322.
(36) Hiyama, T.; Ke, B. *Arch. Biochem. Biophys.* **1971**, *147*, 99.
(37) Gong, X. M.; Agalarov, R.; Brettel, K.; Carmeli, C. *J. Biol. Chem.* **2003**, *278*, 19141.
(38) Xu, W.; Chitnis, P. R.; Valieva, A.; van der Est, A.; Brettel, K.; Guergova-Kuras, M.; Pushkar, Y. N.; Zech, S. G.; Stehlik, D.; Shen, G. Z.; Zybailov, B.; Golbeck, J. H. *J. Biol. Chem.* **2003**, *278*, 27876.
(39) Rava, R. P.; Spiro, T. G. *J. Phys. Chem.* **1985**, *89*, 1856.
(40) Sweeney, J. A.; Asher, S. A. *J. Phys. Chem.* **1990**, *94*, 4784.
(41) Harada, I.; Takeuchi, H. In *Spectroscopy of Biological Systems*; Clark, R. J. H., Hester, R. E., Eds.; Wiley: New York, 1986; Vol. 13; p 157.
(42) Miura, T.; Takeuchi, H.; Harada, I. *Biochemistry* **1988**, *27*, 88.
(43) Hashimoto, S.; Obata, K.; Takeuchi, H.; Needleman, R.; Lanyi, J. K. *Biochemistry* **1997**, *36*, 11583.
(44) Hashimoto, S.; Sasaki, M.; Takeuchi, H.; Needleman, R.; Lanyi, J. K. *Biochemistry* **2002**, *41*, 6495.
(45) Phillips, G. N., Jr.; Teodoro, M. L.; Li, T.; Smith, B.; Olson, J. S. *J. Phys. Chem. B* **1999**, *103*, 8817.
(46) Suydam, I. T.; Boxer, S. G. *Biochemistry* **2003**, *42*, 12050.
(47) Matsuno, M.; Takeuchi, H. *Bull. Chem. Soc. Jpn.* **1998**, *71*, 851.
(48) Fujisawa, T.; Terazima, M.; Kimura, Y. *J. Chem. Phys.* **2006**, 124.
(49) Shoute, L. C. T.; Helburn, R.; Kelley, A. M. *J. Phys. Chem. A* **2007**, *111*, 1251.

JP906491R